10-2012

Multi-objective Optimization of Wind Farm Layouts Under Energy Generation and Noise propagation

Cristina Amon

Wing Yin Kwong

Joaquin Moran

Michael Morgenroth

David Romeo

See next page for additional authors

Authors
Cristina Amon, Wing Yin Kwong, Joaquin Moran, Michael Morgenroth, David Romeo, and Peter Y. Zhang

Proceedings of the ASME 2012 International Design Engineering Technical Conferences & Computers and Information in Engineering Conference
IDETC/CIE 2012
August 12-15, 2012, Chicago, IL, USA

DETC2012-71478

WIND FARM LAYOUT OPTIMIZATION CONSIDERING ENERGY GENERATION AND NOISE PROPAGATION

Wing Yin Kwong
Division of Engineering Science
University of Toronto
Toronto, ON, Canada
penelope.kwong@utoronto.ca

Peter Y. Zhang
Department of Mechanical & Industrial Engineering
University of Toronto
Toronto, ON, Canada
peteryun.zhang@utoronto.ca

David Romero☒
Department of Mechanical & Industrial Engineering
University of Toronto
Toronto, ON, Canada
d.romero@utoronto.ca

Joaquin Moran
Renewable Power Division
Hatch, Inc.
Niagara Falls, ON, Canada
jmoran@hatch.ca

Michael Morgenroth
Renewable Power Division
Hatch, Inc.
Niagara Falls, ON, Canada
mmorgenroth@hatch.ca

Cristina Amon
Department of Mechanical & Industrial Engineering
University of Toronto
Toronto, ON, Canada
cristina.amon@utoronto.ca

ABSTRACT

Wind farm design deals with the optimal placement of turbines in a wind farm. Past studies have focused on energy-maximization, cost-minimization or revenue-maximization objectives. As land is more extensively exploited for onshore wind farms, wind farms are more likely to be in close proximity with human dwellings. Therefore governments, developers, and landowners have to be aware of wind farms' environmental impacts. After considering land constraints due to environmental features, noise generation remains the main environmental/health concern for wind farm design. Therefore, noise generation is sometimes included in optimization models as a constraint. Here we present continuous-location models for layout optimization that take noise and energy as objective functions, in order to fully characterize the design and performance spaces of the optimal wind farm layout problem. Based on Jensen's wake model and ISO-9613-2 noise calculations, we used single- and multi-objective genetic algorithms (NSGA-II) to solve the optimization problem. Preliminary results from the bi-objective optimization model illustrate the trade-off between energy generation and noise production by identifying several key parts of Pareto frontiers. In addition, comparison of single-objective noise and energy optimization models show that the turbine layouts and the inter-turbine distance distributions are different when considering these objectives individually. The relevance of these results for wind farm layout designers is explored.

INTRODUCTION

Wind energy installation has experienced a tremendous increase in the past decade. The Canadian Wind Energy Association envisioned Canada to have 55 GW of wind energy installation by 2025, equivalent to 20% of the country's energy needs [1]. The United States has seen annual growth between 5 and 10 GW since 2007, with a total installed capacity of 43GW through the 3rd quarter of 2011 [2].

Wind energy is still facing resistance in North America due to health and environmental concerns. The government of Canada has published a series of reports regarding noise generation of wind farms [3–5]. Regardless of whether wind farm noise has negative health impact, it concerns both the developers and the residents near wind farms. Therefore noise is an important factor in wind farm design.

Due to the aerodynamic nature of both energy capture and noise generation, these are usually competing factors, meaning that the more energy we capture with a given set of wind turbines, the more noise it might generate. Many aspects affect the noise generation of wind turbines. On one hand, operation of turbine's mechanical components produces noise. On the other hand, wind flowing through turbine generates another type of noise. The wake interactions between turbines can also change noise level and propagation pattern. Therefore, the faster turbines operate (higher rpm), the more noise they generate. An indirect effect appears when the number of turbines increases in a given area with the goal of increasing the energy capture. In such situations, the average expected distance between the turbines and a noise receiver is bound to decrease, thus increasing the sound level measured at the receiver's location.

Traditionally, wind farm design engineers and researchers have included noise as a constraint in their optimization model [6]. This means that when they considered noise as a design factor, they usually tried to find the wind farm design with maximum energy (or minimum cost per energy), while keeping the noise levels below a certain threshold. There are a few potential limitations to this approach. If the optimization is done manually, as it is typically done in the wind energy industry, wind farm design is an iterative and lengthy process, involving stages of layout design for maximum energy, checks for compliance with environmental restrictions (e.g. noise), and refinement of the layout based on infrastructure considerations. Also, feasible solutions might be scarce, if they exist at all, so that it takes a long time to find an acceptable layout, or decide that the project is not profitable. Feasible solutions, in the optimization sense, refer to the layouts that satisfy all environmental, infrastructure and financial constraints, including the noise regulations. On the other hand, if optimization relies on computer, designers will locate feasible solutions faster, but might focus only on one final solution without getting any insights on the design trade-offs, sensitivity, robustness and other acceptable design alternatives. In summary, there is a need for a computational approach for optimization of noise-constrained wind farm layouts that is capable of (a) finding the optimal solution, as well as a set of feasible solutions with acceptable performance, (b) elucidating the design trade-offs and sensitivity of the solution to changes in the position of individual turbines.

We propose a different approach to this problem. Our approach considers both noise minimization and energy maximization as objectives, using a stochastic optimization algorithm, namely Genetic Algorithms. This way, we hope to identify whether noise and energy generation are truly competing factors; and if so, what the relationship between noise and energy is. In addition, by analysing the populations of solutions generated by the Genetic Algorithm, we can gain insights into characteristics of layouts that are associated with good performance. In other words, our goal in using this approach is to understand the trade-off between energy and noise in wind farm layout design and to assist engineers in formulating design guidelines.

Previous Work

Among the recent research work in wind farm design, we are most interested in developments in wind farm optimization models and algorithms. In the following, we describe briefly some developments on these two aspects.

The first study in wind farm layout optimization can be traced back to Mosetti et al. [7], who used a 2.0 km by 2.0 km square to represent the available land. This land was divided into a 10 by 10 grid of square cells, each cell with the side length of five turbine diameters. Turbines could only be placed in the centre of a grid, thus enforcing design guidelines that prescribe minimum separation distance between turbines. The authors captured turbine interactions with the Jensen wake model [8], which considers a linearly-expanding wake, resulting in a downstream wind speed that is a non-linear function of downstream distance. As optimization algorithm, the authors used Genetic Algorithms [9], which has been by far the most commonly used method in the literature. Grady et al. [10] further explored GAs as a solution method, using larger populations and number of generations than previous work, thus leading to better solutions, Emami et al. [11] and González et al. [12] have further improved over Mosetti's approach.

More comprehensive models have been proposed recently. Kusiak and Song [13] solved the turbine layout problem with a continuous-location model, in which turbines were allowed to reside anywhere within the wind farm. Minimum turbine proximity and wind farm boundary were the only constraints, which were then converted into a second objective function. Réthoré et al. [14] explored optimization for offshore wind farm, including an improved cost model in the calculation of the unit cost of energy, which they used as the optimization objective. Saavedra-Morreno et al. [15] incorporated a wind regime that considers spatial difference in wind speeds. In other words, instead of using a single wind speed/direction, or a statistical distribution of wind speed of directions, their model considers the spatial distribution of the wind field.

Réthoré et al. [16] also used a discrete-location approach. However, they employed a two-stage model with increasing resolution of the wind farm. In the second stage, the authors also included more comprehensive cost and revenue models, and increased the number of directions and speeds for wind resources. Chowdhury et al. [17], [18] investigated how the key factors, such as land configuration, influence the wind farm performance. Finally, another recent development on the modelling side is the work of González et al. [12], who include infrastructure considerations in the layout design, such as the cost of foundations and the cost of auxiliary inner roads connecting turbines.

On the algorithmic side of the problem, different methods have been explored. Metaheuristics such as Genetic Algorithms and Particle Swarm Optimization [19] have been extensively applied to the wind farm optimization problem [7], [10], [20], [21], with success. Approaches that combine deterministic search and stochastic search, such as the Extended Pattern Search (EPS) approach of Du Pont and Cagan [22] have also been proposed. In EPS, each turbine in the layout is moved according to a pre-established pattern, with a step size that decreases as the optimization progresses. Turbine moves that lead to an increase in energy production are kept, while those that do not are discarded. This heuristic strategy's rejection-sampling approach is guaranteed to improve upon the initial solution, although there are no guarantees of global convergence.

Donovan [23] [24] and Fagerfjäll [6] explored Mixed-Integer Programming (MIP) models, and solved these problems with traditional branch-and-bound methods. Unlike GAs and other metaheuristics, MIP solvers are included in many operations research software packages, e.g., IBM ILOG CPLEX, and have well-studied convergence behaviours. However, these solvers are not always suited for non-linear, non-convex optimization problems, as the wind farm layout problem is. In fact, both Donovan and Fagerfjäll used an approximate, simplified calculation of energy capture in order to justify their use of MIP solvers.

Common threads across all these applications are: (a) similar objective functions: maximum energy capture, minimum cost of energy, or a weighted sum of energy capture and cost, (b) a pre-determined number and type of turbines, and (c) minimum turbine proximity and convex-polygonal wind farm boundaries as the only optimization constraints.

On a broader scope, in our future work we intend to solve the full-scale, comprehensive wind farm layout optimization problem, including major aspects of the problem: Energy capture, environmental impact and cost. As a first step towards that vision, in this paper we will focus on understanding the energy-noise trade-off in wind farm layout design.

The remainder of this paper is organized as follows. In the following section, we describe the models we used to predict energy capture and noise generation/propagation in the wind farm. Then, we present a brief description of the optimization method used in this work, namely the multi-objective genetic algorithm with fitness assignment by non-dominated sorting. Then, we present our test case, followed by our results in two aspects: (a) validation of our models against industrial-grade software, and (b) single- and multi-objective optimization. We close with our concluding remarks and a discussion of future work.

WIND FARM MODELLING

Wake Modelling

An analytical, closed-form wake model is used to quantify the aerodynamic interaction between turbines. This model was first proposed by Jensen [8], who developed it by considering that momentum is conserved within the wake, and that the wake region expands linearly in the direction of the flow, as shown in Fig. 1.

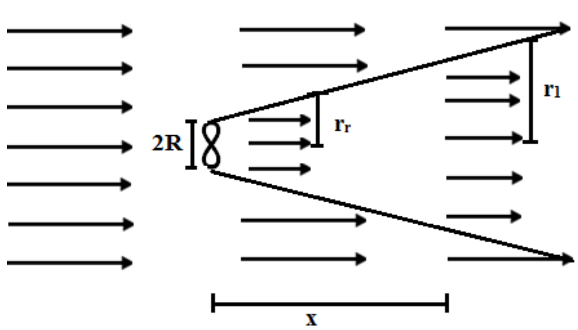

Fig. 1. Schematic representation of Jensen's wake model.

To determine the effective wind speed experienced by a turbine located within another turbines wake, the momentum balance equation can be written

$$\pi r_r^2 u_r + \pi(r_1^2 - r_r^2)u_o = \pi r_1^2 u \qquad (1)$$

where r_r is the turbine rotor radius, r_1 is the radius of the wake at any position x measured downstream, u_o is the free stream wind speed, u_r is the wind speed immediately behind the rotor, and u is the speed of wake a downstream distance x.

According to Betz's theory [25], the wind speed immediately behind the rotor is approximately 1/3 of the free stream speed, and with the assumption of a linearly expanding wake, the downstream speed can be calculated as

$$u = u_o\left(1 - \frac{2}{3}\left(\frac{r_r}{r_1}\right)^2\right) \qquad (2)$$

where r_r is the turbine rotor radius, and r_1 can be found from the following linear relationship representing the wake radius

$$r_1 = r_r + \alpha x \qquad (3)$$

In Eq. (3), α is the entrainment constant, also known as the wake decay constant, and is calculated (empirically) as

$$\alpha = \frac{0.5}{ln\left(\frac{z}{z_o}\right)} \qquad (4)$$

where z is the hub height and z_o is the surface roughness of the terrain, both in metres. Fig. 2 shows the variation of wind speed as a function of position along the wake's centerline. Note the nature of the decay in wind speed, and the rate at which it recovers its free stream value.

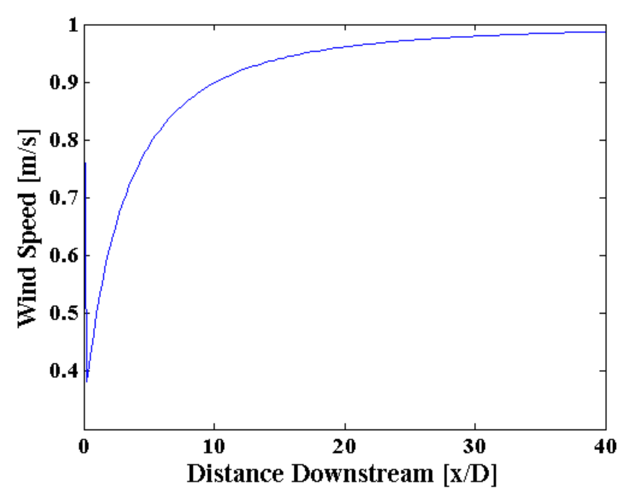

Fig. 2. Wind speed along a single wake's centerline, as a function of distance normalized with the turbine diameter.

For turbines under the influence of multiple wakes, an effective wind speed can be calculated from the sum of kinetic energy deficits from upstream turbines. Note that this is a superposition approach that assumes that kinetic energy deficits can be aggregated. Although this is a simplification of the complex fluid dynamics involved in wake merging, this approach has been used extensively in previous work, especially for optimization purposes, and it is still used in commercial software for wind farm design. For more complex models of wake dynamics, the reader can refer to [26]. The effective speed of the turbine inside n wake regions can therefore be expressed as

$$u = u_o\left[1 - \sqrt{\sum_{i=1}^{n}\left(1 - \frac{u_i}{u_o}\right)^2}\right] \quad (5)$$

Based on the effective wind speed at the turbine rotor, the power produced by the turbine can be calculated through the manufacturer-supplied power curve. Without loss of generality, in this work we follow previous work [7], [10], [22] and use a simplified expression for a turbine's power production: power is a simple continuous function of the local effective speed at hub height. Hence, when the farm is subjected to a uniform wind speed, the total power extracted from n wind turbines is expressed in the following equation:

$$P_{tot} = \sum_{i=1}^{N} \frac{1}{3} u_i^{\,3} \qquad (6)$$

Finally, we note that the annual energy production (AEP) of wind farm is defined as the integration of power production (kW) over time (h). This is an expected value of a random variable, as it is based on the probability distribution of wind speeds and directions. Hence, it is calculated as

$$AEP = 8766 \sum_i \sum_j \sum_k F_{ijk} P_{ijk} \qquad (7)$$

where i, j and k are indices over the number of wind directions, speeds and the number of turbines, respectively, F_{ijk} is the probability of wind coming at speed u_i from direction θ_j at turbine location k, and P_{ijk} is the corresponding power generated by that turbine, in kW. Finally, 8766 is the average number of hours in a year, including leap years.

Noise Modelling

In the context of the ISO-9613-2 standard [27], receptors are the locations where the sound level is to be measured or predicted. In wind farm layout design, all human settlings located within the wind farm terrain, or within a certain neighbourhood, are considered receptors for noise calculation purposes.

In a practical setting, the equivalent continuous downwind octave-band sound pressure level (SPL) at each receptor location is calculated for each point source, at each of the eight octave bands with nominal mid-band frequencies from 63 Hz to 8 kHz [27],

$$L_f = L_W + D_c - A \qquad (8)$$

where L_w is the octave-band sound power emitted by the source, D_c is the directivity correction for sources that are not omni-directional, A is the octave-band attenuation, and f is a subscript indicating that this quantity is calculated for each octave band.

Several octave-band weightings are available to convert the sound pressure levels in Eq. (8) to an effective SPL. For wind farm layout applications, it is customary to use A-weighted sound pressure levels [4]. The equivalent continuous A-weighted downwind sound pressure level at specific location can be calculated from summation of contributions of each point sound source at each octave band,

$$L_{avg} = 10\, log\left\{\sum_{i=1}^{n}\left[\sum_{j=1}^{8} 10^{0.1\left[L_f(i,j)+A_f(j)\right]}\right]\right\} \quad (9)$$

where n is the number of point sound sources, j is the index representing one of the eight standard octave-band mid-band frequencies, and the $A_f(j)$ are the standard A-weighting coefficients.

The attenuation term (A) in Eq. (8) is the sum of different attenuation effects

$$A = A_{div} + A_{atm} + A_{gr} + A_{bar} + A_{misc} \quad (10)$$

due to geometrical divergence (A_{div}), atmospheric absorption (A_{atm}), ground effects (A_{gr}), sound barriers (A_{bar}) and miscellaneous effects (A_{misc}). In this model, it is assumed that the attenuation due to sound barriers and miscellaneous effects are insignificant. Further detail of the calculation procedure can be found in the ISO 9613-2 document [27]. An illustration of the behaviour of the SPL as a function of (radial) distance with respect to the source is shown in Fig. 3.

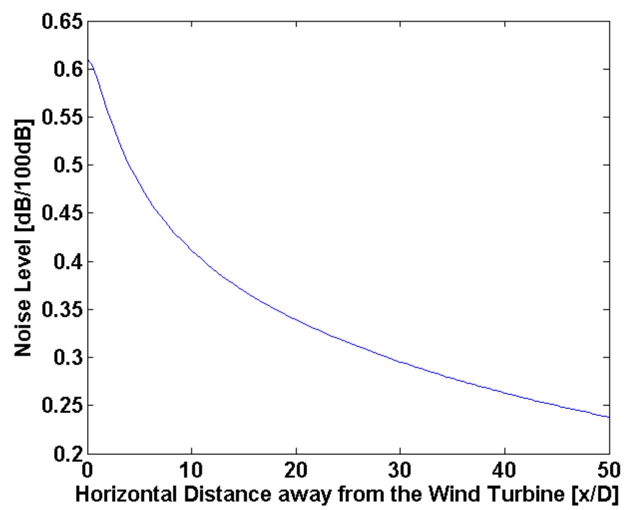

Fig. 3. Sound Pressure Level (A-weighted) as a function of distance from the source.

OPTIMIZATION WITH GENETIC ALGORITHMS

Genetic algorithms (GAs) [9] are probabilistic search algorithms inspired by the concept of natural selection and survival of the fittest. GAs search through the solution space by keeping a population (set) of solutions, which are ranked according to their fitness to solve the optimization problem (e.g. objective function values), and evolved through many generations. Due to their probabilistic nature, GAs are complete search methods, meaning that they can perform an exhaustive search of the input space if they are run for long enough, as long as the elitism and mutation operators are implemented with non-zero probability. In other words, GAs are guaranteed to converge to the neighbourhood of the global optima, but they can take an arbitrarily large number of function evaluations (i.e. run time) to do so.

An important advantage of GAs is that they do not require information about the gradient of the solutions, therefore avoiding problems with the and non-continuity of the solution space. This characteristic of GAs makes them well suited for the wind farm layout problem. On the other hand, GAs typically exhibit slow rates of convergence, thus increasing the computation cost and runtime of the optimization. In this work, we will not focus on improving the runtime behaviour and/or convergence rate of the algorithm. Rather, we will exploit its advantages to characterize the design space of the wind farm layout.

There are several variants GAs that are suited for Multi-Objective Optimization (MOO) problems, such as the Strength-Pareto Evolutionary Algorithm (SPEA, SPEA-2) [28], [29], and the Non-Domination Sorting Genetic Algorithm (NSGA, NSGA-II) [30], [31], among others [32]. Both SPEA-2 and NSGA-II have been shown to have similar performance over an array of test functions. This is expected since the algorithms are very similar, the main difference being the method used to convert multiple objective function values to a unique metric of fitness. In this work, we use the NSGA-II algorithm; its main steps are shown in Fig. 4.

In the wind farm layout problem, n_{pop} initial layout patterns are generated randomly, and the corresponding objective values (energy generation, noise level) are evaluated. For each individual in the population, a rank is assigned according to their non-domination status (Non-Dominated Sort) and the distance between the solution and its neighbours in the objective space (Crowding Distance). In the Parent Selection stage, parents for the next generation are chosen based on the rank and the crowding distance via binary tournament. Solutions with lower rank values are preferred, as the ranks are assigned so that the current Pareto front has rank 1. Crowding distance is used as a secondary fitness value to break ties when comparing solutions based on rank. After parents are selected, an offspring generation of size n_{off} is created by crossover and mutation of the layout patterns of the parent generation. After evaluating the objective function values of the offspring population, it is merged with the parent population, and new rank and crowding distance values are assigned. Elitism is implemented by keeping only the best (i.e. rank 1) or the first n_{pop}-best solutions for the next generation (iteration) of the algorithm. The readers are referred to [31] for more details on the algorithm and its implementation.

TEST CASES

Fig. 5 shows the problem scenario with WR1 – a wind regime with only one direction of wind with uniform speed, following Mosetti et al. [7], Grady [10] and others. WR36 is the second set of cases with a more complex wind regime, as described by the probability distribution in Fig. 6. In previous work, a discretized version of the optimization problem was solved by defining a square grid over the wind farm terrain. In this work, we allow turbine positions to vary continuously, to more closely reflect the setting found in layout design practice. Note that we do not enforce proximity constraints in our optimization, as we would like to see them arise naturally from the optimization objectives. In previous work, proximity constraints were enforced, either directly as actual constraints, or indirectly using the discrete version of the problem.

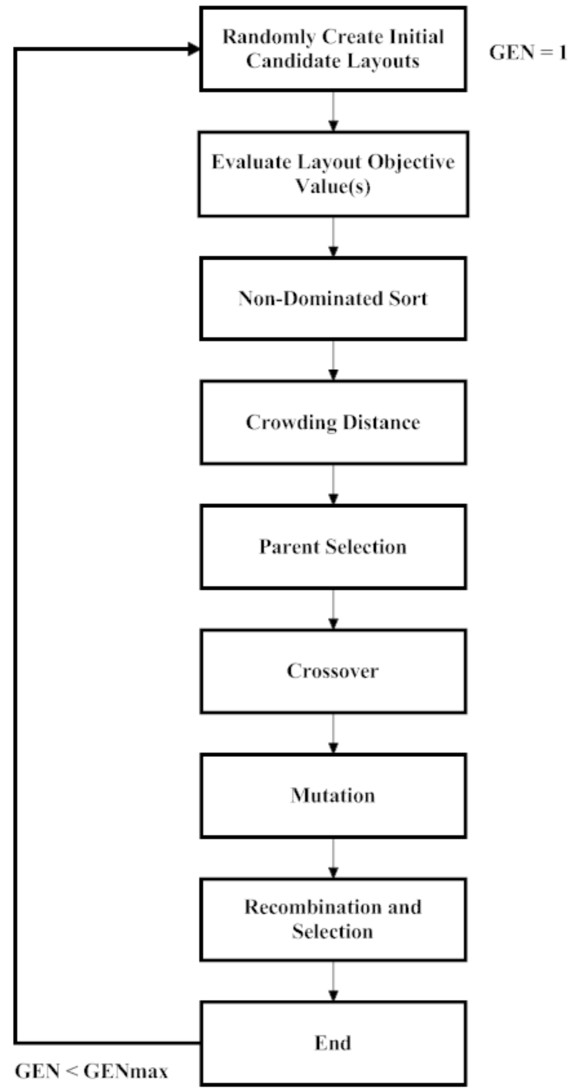

Fig. 4. Main steps in NSGAII.

Following previous work, in our test case, the wind farm is a piece of flat terrain, with dimensions of 2.0 km by 2.0 km, subject to a uniform, unidirectional wind speed of 12 m/s. The characteristics of the wind turbines are shown in Table 1, corresponding to typical turbine models used in previous work. The noise generation levels were estimated from the values reported in [33] for turbines of the same rated capacity.

In this work, we examined two optimization objectives. In the first case, we solved the maximum energy problem by finding the optimal location of 15, 30, and 45 turbines within the farm. Due to the stochastic nature of the optimization algorithm, we run this test case 10 times with different random seeds, and report our results either as the best solution out of the runs, the average behaviour, or the aggregate statistical behaviour for the 10 runs.

Second, we solved for the optimal location of 15, 30, and 45 turbines so that the maximum noise (SPL) at the boundary of the wind farm is minimized. The rationale for solving the optimal layout problem by minimizing noise, without consideration of energy generation, is the observation that in practice noise generation is frequently an overriding concern to secure final approval of a wind project. Finally, the MOO problem is solved by maximizing energy generation and minimizing noise at the wind farm's boundary, to illustrate the performance trade-off between these two objectives.

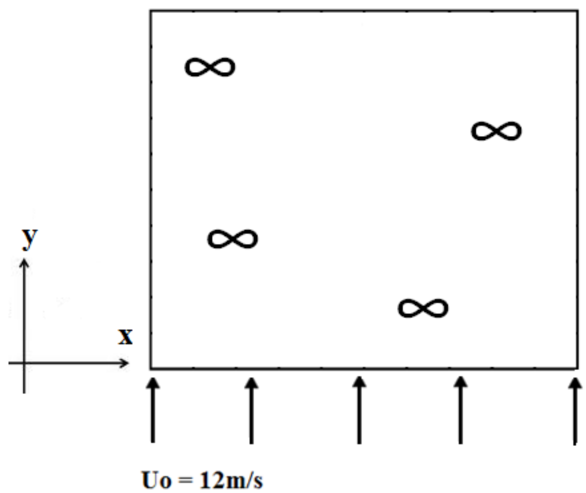

Fig. 5. Schematic representation of test case. Four (4) hypothetical turbines are shown facing the wind.

Table 1. Wind turbine parameters for the test case.

Parameter	Value
Turbine Hub Height (z)	60 m
Terrain Roughness Length (z_0)	0.3 m
Rotor Radius (r_r)	40 m
Power Curve	$0.3u^3$kW
Noise Generation (L_w)	100 dB

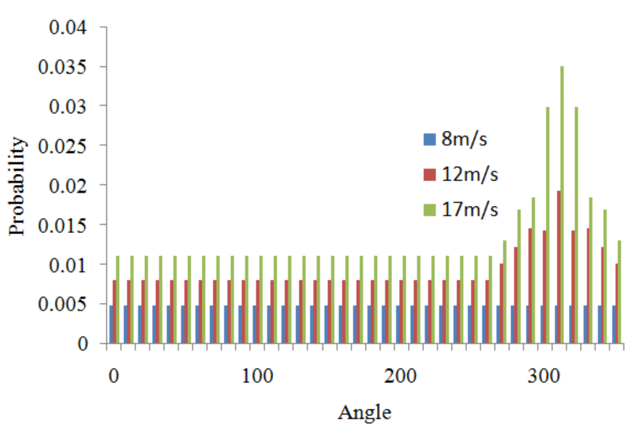

Fig. 6. Distribution of wind speeds and directions for WR36 cases.

Two wind regimes, WR1 and WR36, are tested separately. The first one has a uniform, single-direction wind pointing from south to north at 12 m/s. The latter is described by Fig. 6, which is a probability distribution for wind speed and direction mirrored from previous work [10], [22].

The next section presents our results. First, we comment on the validation of our implementation of the energy and noise models, by comparing our results with previous work and/or an industry-grade, open-source software for wind farm design and analysis, openWind [34]. Then, we present the trade-off surface for the multi-objective, energy-noise optimization. Finally, we compare our results for multi- and single-objective optimizations, and discuss the potential implications for wind farm layout design practice.

PRELIMINARY RESULTS

Validation of the Models

The first task in our optimization effort was the implementation of the wake and noise models for a wind farm. We chose C++ for its computational efficiency.

To validate our implementation, we evaluated the annual energy production (AEP) and maximum noise level of two layouts different number of turbines using (a) our implementation of the models, (b) openWind, an open source, industry-grade software. Table 2 shows the predicted energy performance according to these models, and their difference expressed as a percentage of the openWind prediction, which is assumed to be correct [35]. Fig. 7 shows a comparison of the predicted sound pressure level inside the wind farm terrain. After noting the slight difference in colour map, legend and scale, it can be seen that the predictions are essentially the same.

Table 2. Comparison of Annual Energy Production (AEP) predictions between current implementation and openWind.

	This work	openWind	Difference
30 Turbines, WR1	132.38 GWh	132.17 GWh	0.2%
30 Turbines, WR36	225.88 GWh	230.48 GWh	2.0%

Optimization

Once the models were validated, we focused our efforts on the optimization. Fig. 8 shows the spatial histogram of turbine locations for 10 runs of the multi-objective NSGA-II algorithm. In other words, the figure shows the relative frequency with which one or more turbines were placed on a given cell during the optimization process. Although our optimization approach considers turbine locations to be continuous variables, we have discretized the wind farm terrain in a grid of square cells with side lengths of 100 m. This aids in the presentation of the information, and makes comparisons with previous work easier in the future.

A wind farm designer can extract valuable information from Fig. 8. For example, it is clear that, if the goal of the optimization is to minimize sound levels at the boundary of the farm, optimal layout configurations will tend to have only a few turbines near the boundaries, with a tendency to concentrate towards the centre of the farm. On the other hand, if the focus is on configurations with the maximum energy generation, turbines will tend to spread across the wind farm terrain, including locations along the borders of the farm. In addition, by correlating both figures we can see which land cells are critical to achieve a design that both increases AEP and decreases SPL. In particular, there are several areas (e.g., the centre of Fig. 8(a)) with larger sampling frequencies, meaning that layouts with turbines in these locations tend to perform better according to our optimization objectives. Similar comments can be made for the optimization case with 15 and 30 turbines (not shown).

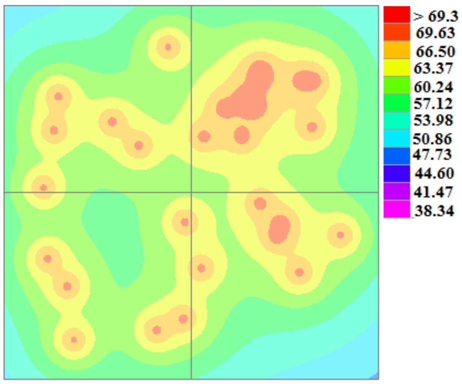

(a)

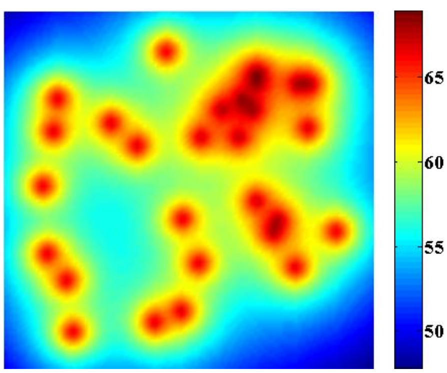

(b)

Fig. 7. Comparison of sound pressure level (SPL) field inside the wind farm: (a) openWind, (b) current implementation.

Note that the spatial histograms used in this work are a novel way of presenting the optimization results. Their usefulness is based on the assumption that, due to the selection procedure implemented in the optimization algorithm, its *long term* sampling distribution provides information about the probability of a given location being part of an optimal layout. This is valuable information for the wind farm developers, as it quantifies the importance of a given piece of land for an optimal wind farm design. In other words, looking at the spatial histograms enables the designer to leverage data generated during the optimization *process*, rather than focusing only on the optimal *solution*. The reader is referred to [36] for previous work that has exploited the ensemble of intermediate solutions to extract additional information from the optimization process.

Fig. 9 shows the (approximate) Pareto front for several numbers of turbines. First, note the convexity of the front, which was expected from the nature of the objective functions and their behaviour; compare, for example, Fig. 2 with Fig. 3. Further tests are underway to check if the observed discontinuities ("holes") in the Pareto front are a feature of the problem or are due to a premature stop of the optimization. In any case, the approximation in Fig. 9 is sufficient to characterize the main features of the trade-off. Second, note that for the case with 15 turbines, the Pareto front does not spread along the horizontal (AEP) axis. This is expected, since in this case only 15 turbines are placed in the farm, and there are many possible layouts that will yield maximum energy, making it unlikely that AEP would be a limiting objective in terms of finding an optimal layout. In other words, it would be difficult to find layouts of 15 turbines with lower energy production, even if they are placed randomly.

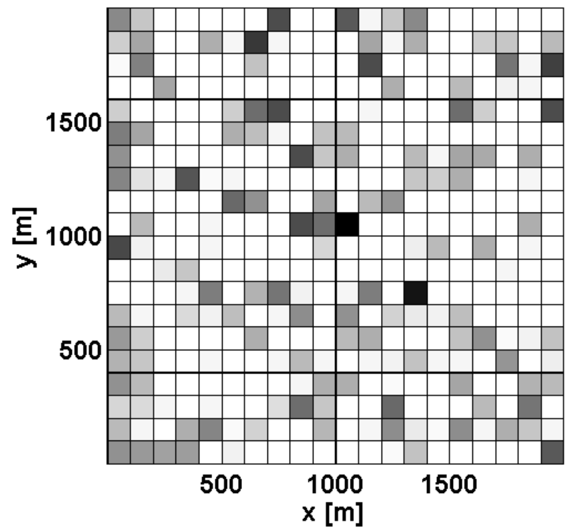

(a)

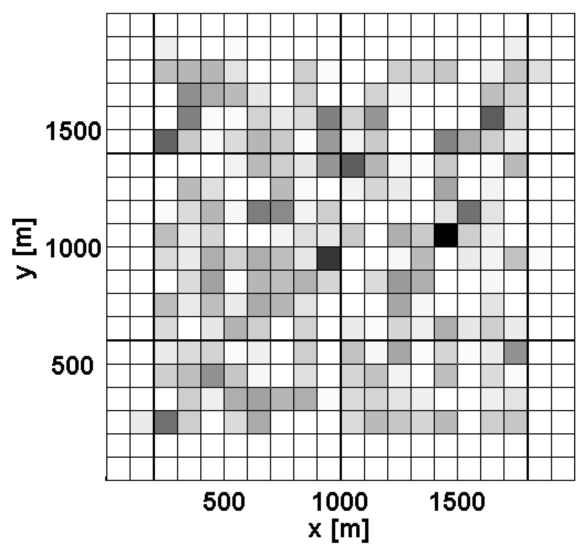

(b)

Fig. 8. Spatial histograms of turbine locations, multi-objective (energy-noise) optimization (WR36, 45 turbines). Data corresponding to all turbines belonging to a layout that has (a) AEP > 3.2E4 GWh, or (b) SPL < 55 dBA. Darker shades indicate higher probability.

An interesting feature of Fig. 9 is the slope of different sections of the Pareto front, indicating regions of very high and very low sensitivity. For example, for the case with 30 turbines, we can see that there is an array of layouts whose noise emissions would be below 50 dBA, while providing energy generations in the range 180-205 GWh. In other words, there are layouts with up to 10% difference in energy production but noise levels below 50 dBA. Similarly, there are many layout options that can produce close to the maximum energy (approx. 225 GWh) at a wide range of noise emissions (58-64 dBA). In addition, there is a short "transition" section, in which we can obtain improvements in energy generation with discrete increases in SPL. Finally, note that as more turbines are added to the wind farm, we observe more spread in energy and smaller spread in noise. From a designer's point of view, this indicates that when adding more turbines, layout designs becomes more important, as it is possible to find a wider range of AEP values for a given noise level constraint.

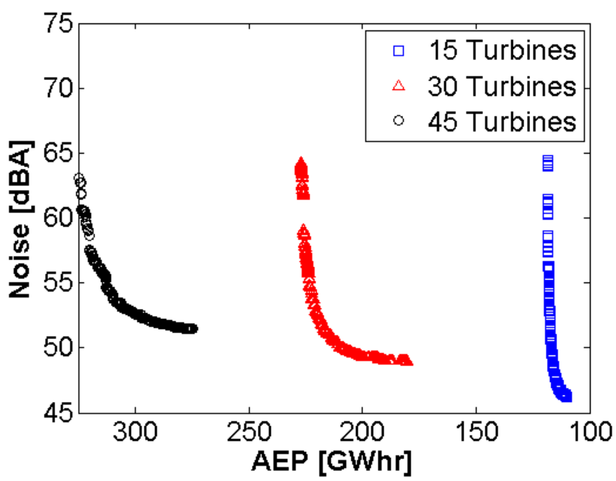

Fig. 9. Pareto fronts for layouts with (a) 15, (b) 30, and (c) 45 turbines, WR36.

As part of our continuing work, we are trying to study the fundamental differences between solutions based on energy maximization and those based on noise minimization only. For example, Fig. 10 shows the spatial histograms of turbine locations for these single-objective optimizations. Again, each cell in the wind farm terrain is considered a histogram bin, so Fig. 10 is generated by counting the number of times that a turbine was placed within the cell, based on the final population of the ten GA optimization runs. Note that in both cases shown in Fig. 10, all regions of the wind farm were sampled for potential turbine locations by the optimization algorithm, as indicated by absence of cells coloured in white. Although more tests are needed, we can notice differences in the spatial distribution of the turbines, from which we hope to extract design rules.

As an additional characterization of the similarity of the solution and trade-offs, we tried to determine if a particular spacing between turbines would favour one optimization objective or the other. For this aspect of the study, we have created histograms of inter-turbine distances, measured in both down-wind and cross-wind directions for the WR1 case, shown in Fig. 11 and Fig. 12. Note that we did not implement any turbine proximity constraint in our optimization, precisely to be able to observe this behaviour. This preliminary results show that, compared with noise-minimization, energy-maximization introduced more spread-out layouts, in both downwind and crosswind directions. As these are preliminary results, we are currently in the process of analysing the data further.

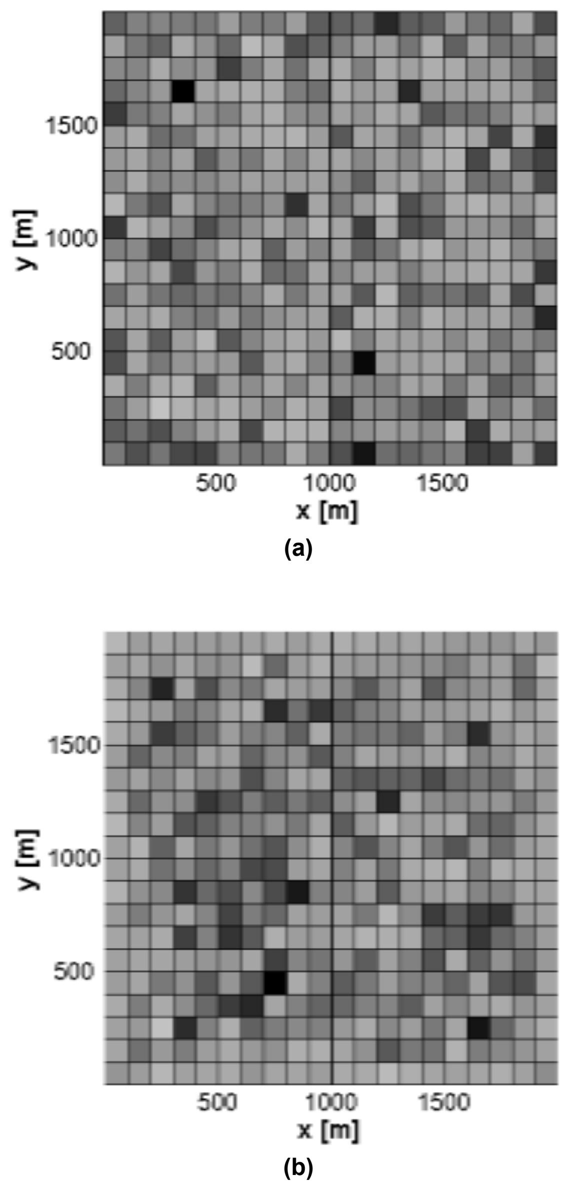

Fig. 10. Spatial histograms of turbine locations, single-objective optimization (WR36, 30 turbines). (a) Maximum energy, (b) Minimum noise.

CONCLUSION

In this work, we have conducted single- and multi-objective wind farm layout optimization studies, considering maximum energy generation and minimum noise levels at the boundary of the wind farm as objectives.

After validating our models for energy and noise against industry-grade wind farm analysis software, we obtained the (approximate) Pareto frontier for the multi-objective problem.

In addition, we analyzed the results from the optimization process from a statistical point of view. By noting that the stochastic optimization algorithm (GA, NSGA-II) samples more frequently the regions of the input space that are associated with optimal solutions, we created spatial histograms of turbine locations sampled during the optimization. Finally, we created histograms of inter-turbine distances, with the goal of inferring design rules that can guide practicing wind farm engineers.

Preliminary results of our study show a convex Pareto frontier with three distinct areas. First, there is a set of solutions that result in the largest energy values at a wide range of noise levels. Second, there is a set of solutions that provide low noise levels while resulting in a wide range of energy values. Finally, there is a small, intermediate region where a trade-off can be seen between noise and energy. In addition, we observed important differences in the Pareto fronts, regarding the relative importance of the energy and noise objectives in finding solutions for the layout problem. In particular, as more turbines are added to the farm, we observed a larger spread in annual energy production (AEP) values with a smaller spread in sound pressure level (SPL) values, indicating that a shift in design priorities may be warranted.

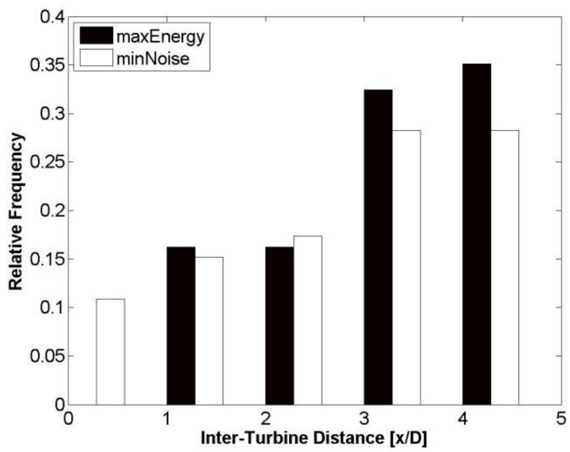

Fig. 11. Histogram of inter-turbine distances, downwind direction (WR1, 30 turbines).

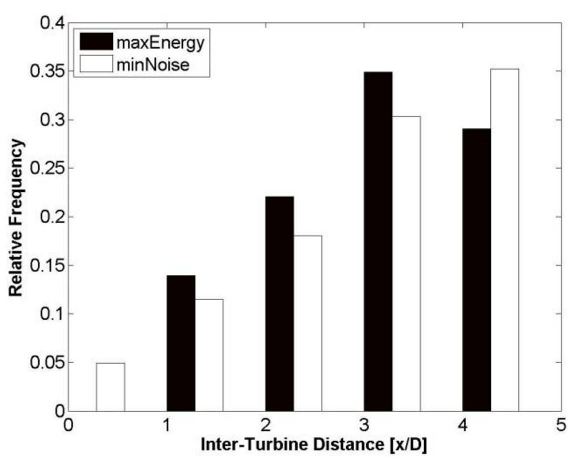

Fig. 12. Histogram of inter-turbine distances, crosswind direction (WR1, 30 turbines).

Regarding the layouts associated with different areas of the Pareto frontier, our preliminary results show that the turbine layouts and the inter-turbine distance distributions are different when considering these objectives individually. Of particular relevance for wind farm designers is the determination of sampling frequencies for different areas of the wind farm terrain. Such analysis provides important information regarding the areas of the wind farm that are important for obtaining optimal layouts in the single- or multi-objective scenarios.

Our work will focus, in the immediate future, on comparing our results with previous work from Mosetti et al. [7], Grady et al. [10] and Du Pont et al. [22], and on extending our analysis to consider multiple wind directions, speeds and a wider range of numbers of turbines to fully describe the optimal design problem. Statistical analysis of the differences in the layouts and inter-turbine distances will also be conducted.

REFERENCES

[1] Canadian Wind Energy Association, “Wind Vision 2025.”

[2] American Wind Energy Association, “Industry Statistics,” 2012. [Online]. Available: http://www.awea.org/learnabout/industry_stats/index.cfm . [Accessed: 12-Feb-2012].

[3] Chief Medical Officer of Health (CMOH) of Ontario, “The Potential Health Impact of Wind Turbines,” 2010.

[4] Ministry of the Environment (Canada), “Noise Guidelines for Wind Farms,” 2008.

[5] Ministry of the Environment (Canada), “Compliance Protocol for Wind Turbine Noise - Guideline for Acoustic Assessment and Measurement,” 2011.

[6] P. Fagerfjäll, “Optimizing wind farm layout – more bang for the buck using mixed integer linear programming,” Chalmers University of Technology and Gothenburg University, 2010.

[7] G. Mosetti, C. Poloni, and B. Diviacco, “Optimization of wind turbine positioning in large windfarms by means of a genetic algorithm,” *Journal of Wind Engineering and Industrial Aerodynamics*, vol. 51, no. 1, pp. 105-116, Jan. 1994.

[8] N. O. Jensen, “A note on wind generator interaction,” 1983.

[9] J. H. Holland, *Adaptation in natural and artificial systems*. Ann Arbour: Univ. of Michigan Press, 1975.

[10] S. Grady, “Placement of wind turbines using genetic algorithms,” *Renewable Energy*, vol. 30, no. 2, pp. 259-270, Feb. 2005.

[11] A. Emami and P. Noghreh, “New approach on optimization in placement of wind turbines within wind farm by genetic algorithms,” *Renewable Energy*, vol. 35, no. 7, pp. 1559-1564, Jul. 2010.

[12] J. S. González, A. G. Gonzalez Rodriguez, J. C. Mora, J. R. Santos, and M. B. Payan, "Optimization of wind farm turbines layout using an evolutive algorithm," *Renewable Energy*, vol. 35, no. 8, pp. 1671-1681, Aug. 2010.

[13] A. Kusiak and Z. Song, "Design of wind farm layout for maximum wind energy capture," *Renewable Energy*, vol. 35, no. 3, pp. 685-694, Mar. 2010.

[14] P.-E. Réthoré, P. Fuglsang, G. C. Larsen, T. Buhl, T. J. Larsen, and H. A. Madsen, "TopFarm : Multi-fidelity Optimization of Offshore Wind Farm," *Wind Energy*, no. 2007, 2010.

[15] B. Saavedra-Moreno, S. Salcedo-Sanz, a. Paniagua-Tineo, L. Prieto, and a. Portilla-Figueras, "Seeding evolutionary algorithms with heuristics for optimal wind turbines positioning in wind farms," *Renewable Energy*, vol. 36, no. 11, pp. 2838-2844, Nov. 2011.

[16] P.-E. Réthoré, P. Fuglsang, G. C. Larsen, T. Buhl, T. J. Larsen, and H. A. Madsen, "TopFarm : Multi-fidelity Optimization of Offshore Wind Farm," in *Proceedings of the Twenty-first (2011) International Offshore and Polar Engineering Conference*, 2011, vol. 8, no. 2007.

[17] S. Chowdhury, J. Zhang, A. Messac, and L. Castillo, "Unrestricted wind farm layout optimization (UWFLO): Investigating key factors influencing the maximum power generation," *Renewable Energy*, vol. 38, no. 1, pp. 16-30, Feb. 2012.

[18] S. Chowdhury, J. Zhang, A. Messac, and L. Castillo, "Characterizing the influence of land configuration on the optimal wind farm performance," in *Proceedings of the ASME 2011 International Design Engineering Technical Conferences & Computers and Information in Engineering Conference*, 2011.

[19] J. Kennedy and R. Eberhart, *Particle swarm optimization*. IEEE, pp. 1942-1948.

[20] C. Wan, J. Wang, G. Yang, and X. Zhang, "Optimal Micro-siting of Wind Farms by Particle Swarm Optimization," *Lecture Notes in Computer Science*, vol. 6145, pp. 198-205, 2010.

[21] M. Bilbao and E. Alba, "Simulated Annealing for Optimization of Wind Farm Annual Profit," *2009 2nd International Symposium on Logistics and Industrial Informatics*, vol. 0, no. 2, pp. 1-5, Sep. 2009.

[22] B. L. Du Pont and J. Cagan, "An Extended Pattern Search Approach to Wind Farm Layout Optimization," *ASME Conference Proceedings*, vol. 2010, no. 44090, pp. 677-686, 2010.

[23] S. Donovan, G. Nates, H. Waterer, and R. Archer, "Mixed Integer Programming Models for Wind Farm Design Columbia University , New York City," *New York*. New York City, 2008.

[24] S. Donovan, "An improved mixed integer programming model for wind farm layout optimisation," in *Proceedings of the 41th Annual Conference of the Operations Research Society*, 2006, pp. 143-151.

[25] J. F. Manwell, J. G. McGowan, and A. L. Rogers, "Chapter 3 - Aerodynamics of Wind Turbines," in *Wind Energy Explained*, 2009.

[26] P.-E. Réthoré, "Wind Turbine Wake in Atmospheric Turbulence," Aalborg University, 2009.

[27] "Acoustics - Attenuation of sound during propagation outdoors - Part 2: General method of calculation (ISO 9613-2:1996)."

[28] E. Zitzler and L. Thiele, "Multiobjective evolutionary algorithms: a comparative case study and the strength Pareto approach," *IEEE Transactions on Evolutionary Computation*, vol. 3, no. 4, pp. 257-271, 1999.

[29] E. Zitzler, M. Laumanns, and L. Thiele, "SPEA2: Improving the Strength Pareto Evolutionary Algorithm for Multiobjective Optimization," in *Evolutionary Methods for Design, Optimisation and Control with Application to Industrial Problems (EUROGEN 2001)*, 2001, pp. 95-100.

[30] N. Srinivas and K. Deb, "Muiltiobjective Optimization Using Nondominated Sorting in Genetic Algorithms," *Evolutionary Computation*, vol. 2, no. 3, pp. 221-248, Sep. 1994.

[31] K. Deb, A. Pratap, S. Agarwal, and T. Meyarivan, "A fast and elitist multiobjective genetic algorithm: NSGA-II," *IEEE Transactions on Evolutionary Computation*, vol. 6, no. 2, pp. 182-197, Apr. 2002.

[32] E. Zitzler, K. Deb, and L. Thiele, "Comparison of multiobjective evolutionary algorithms: empirical results.," *Evolutionary computation*, vol. 8, no. 2, pp. 173-95, Jan. 2000.

[33] A. L. Rogers and J. F. Manwell, "Wind Turbine Noise Issues," Amherst, 2004.

[34] "openWind." AWS Truepower, Albany, NY, 2011.

[35] "OpenWind Theoretical basis and Validation." AWS Truepower, Albany, NY, 2010.

[36] M. Sambridge, "Geophysical inversion with a neighbourhood algorithm-II. Appraising the ensemble," *Geophysical Journal International*, vol. 138, no. 3, pp. 727-746, Sep. 1999.